Colloids and Surfaces B: Biointerfaces 117 (2014) 199–205

Contents lists available at ScienceDirect

Colloids and Surfaces B: Biointerfaces

journal homepage: www.elsevier.com/locate/colsurfb

Facile green extracellular biosynthesis of CdS quantum dots by white rot fungus *Phanerochaete chrysosporium*

Guiqiu Chen[a,b,*], Bin Yi[a,b], Guangming Zeng[a,b,*], Qiuya Niu[a,b], Ming Yan[a,b], Anwei Chen[a,b], Jianjian Du[a,b], Jian Huang[a,b], Qihua Zhang[a,b]

[a] College of Environmental Science and Engineering, Hunan University, Changsha 410082, PR China
[b] Key Laboratory of Environmental Biology and Pollution Control (Hunan University), Ministry of Education, Changsha 410082, PR China

ARTICLE INFO

Article history:
Received 17 July 2013
Received in revised form 14 January 2014
Accepted 17 February 2014
Available online 24 February 2014

Keywords:
CdS
Nanoparticles
Biosynthesis
Face-centered cubic

ABSTRACT

This study details a novel method for the extracellular microbial synthesis of cadmium sulfide (CdS) quantum dots (QDs) by the white rot fungus *Phanerochaete chrysosporium*. *P. chrysosporium* was incubated in a solution containing cadmium nitrate tetrahydrate, which became yellow from 12 h onwards, indicating the formation of CdS nanocrystals. The purified solution showed a maximum absorbance peak between 296 and 298 nm due to CdS particles in the quantum size regime. The fluorescence emission at 458 nm showed the blue fluorescence of the nanoparticles. X-ray analysis of the nanoparticles confirmed the production of CdS with a face-centered cubic (fcc) crystal structure. The average grain size of the nanoparticles was approximately 2.56 nm, as determined from the full width at half-maximum (FWHM) measurement of the most intense peak using Scherer's equation. Transmission electron microscopic analysis showed the nanoparticles to be of a uniform size with good crystallinity. The changes to the functional groups on the biomass surface were investigated through Fourier transform infrared spectroscopy. Furthermore, the secretion of cysteine and proteins was found to play an important role in the formation and stabilization of CdS QDs. In conclusion, our study outlines a chemical process for the molecular synthesis of CdS nanoparticles.

1. Introduction

Semiconductor nanoparticles known as quantum dots (QDs), which possess unique electronic and optical properties owing to quantum confinement effects [1,2], have recently gained attention. In the past twenty years, practical applications of QDs of various sizes, shapes, and compositions [3–6] have been widely explored; QDs have been used as biological fluorescence markers [7,8] and have been employed in the production of optoelectronic transistor components [9] and solar batteries [10]. Among the various QDs, the properties of cadmium sulfide (CdS) nanocrystals (such as a tunable size-dependent emission within the entire visible range) have led to an increasing interest in energy [11,12], magnetics [13], and biomedical applications [14]. In comparison to conventional fluorescent dyes, CdS QDs have the advantages of high photostability, controllable and narrow emission bands, and a high quantum yield. CdS QDs have also been widely utilized in the bioimaging of living cells [15–17].

To date, nanocrystals have been synthesized by various chemical and physical methods; however, most chemical methods cannot avoid the addition of toxic chemicals [18,19], fuelling a pressing need for developing environmentally friendly processes for nanoparticle synthesis. Biological methods for nanoparticle synthesis using either microbes or plant extracts have provided reliable, environmentally friendly, and less toxic alternatives to chemical and physical processes [20]. Presently, the use of some biological templates, including carbohydrates [21], peptides [22], nucleotides [23], and fusion proteins [24], has been advocated for nanocrystal synthesis. Such bionic approaches for the synthesis of nanocrystals may be extended to living biological systems [25–28], which contain ideal endogenous nano-structured templates for the design and synthesis of nanomaterials owing to their inherent ability for molecular recognition and self-assembly [29,30].

Recently, microorganisms such as bacteria, yeast, and fungi have played an important role in the remediation of toxic metals through the reduction of metal ions, generating interest as 'nanofactories'. The bacterium *Bacillus licheniformis* has been reported to be an excellent microbial resource for the extracellular synthesis of

* Corresponding authors at: College of Environmental Science and Engineering, Hunan University, Changsha 410082, PR China. Tel.: +86 731 88822829; fax: +86 731 88823701.
E-mail addresses: gqchen@hnu.edu.cn (G. Chen), zgming@hnu.edu.cn (G. Zeng).

http://dx.doi.org/10.1016/j.colsurfb.2014.02.027
0927-7765/

gold nanocubes [31], while silver nanoparticles have been synthesized by *Phanerochaete chrysosporium* [32], *Puccinia graminis* [33], and *Klebsiella pneumonia* [34–36]. The preparation of cadmium telluride (CdTe) QDs with tunable fluorescence emissions by *Escherichia coli* has been reported [37]. Various microorganisms such as *Fusarium oxysporum* [38], *Schizosaccharomyces pombe* [39], *Rhodopseudomonas palustris* [40], *Coriolus versicolor* [41], and *E. coli* [42] have been used to synthesize CdS QDs. Moreover, the preparation of ZnS nanoparticles by sulfate-reducing bacteria under anaerobic conditions, and by *Rhodobacter sphaeroides*, has also been reported [43].

These methodologies have been applied at ambient temperature and are considered eco-friendly and less toxic compared to conventional physical and chemical methods. However, similarly to other synthetic methods, microbial synthesis presents several challenges that remain unaddressed, such as improved control over size and shape, and scale-up of the process for bulk preparations. Another challenge faced by microbial techniques is the elucidation of the synthesis mechanism at the molecular level, which may eventually foster better control over size, shape, composition, crystallinity, and monodispersity.

In the present study, we established a new method for synthesis of fluorescent QDs by manufacturing CdS QDs using *P. chrysosporium*. The method allowed one-step preparation of CdS QDs from Cd and S precursors. The morphology and crystallinity of the biosynthesized CdS QDs was measured by transmission electron microscopy (TEM) and X-ray diffraction (XRD). The stability was determined by thermogravimetric and differential thermal analysis (TG/DTA). The optical properties were determined by ultraviolet–visible (UV–vis) and photoluminescence (PL) spectra. Furthermore, Fourier transform infrared spectroscopy (FTIR) was used to investigate the possible mechanism of the synthesis. The study provides an economical and eco-friendly approach to the fabrication of fluorescent biocompatible CdS QDs that possess superior optical properties.

2. Materials and methods

2.1. Materials

Thioacetamide (TAA, 99%) was purchased from Tianjin Kermel Chemical Reagent Co. Ltd. (China) and mercaptoacetic acid (TGA, 90%) was obtained from Sinopharm Chemical Reagent Co. Ltd. (China). Cadmium nitrate tetrahydrate (99%) was purchased from Tianjin Guangfu Fine Chemical Research Institute (China). All other reagents used were of analytical grade and used without further purification. The water was deionized through an ultra-pure water machine (UPT-II-40, China).

2.2. Fungal culture

The white rot fungal strain *P. chrysosporium* (BKMF-1767) was obtained from the Chinese Typical Culture Center of Wuhan University. The strain was maintained at 4 °C on potato-dextrose agar plates. The fungus was cultivated in Kirk inorganic liquid medium in Erlenmeyer flasks (500 mL) using the shake flask method. The flask was filled with 200 mL of the growth medium that had been autoclaved at 105 °C for 30 min and cooled to room temperature before use. The pH after autoclaving was 7.0.

The inoculum was prepared by scraping some *P. chrysosporium* spores from a single fungal colony growing on a dextrose-potato agar plate and slowly adding them to bacteria-free water until the turbidity (WGZ-1, China) of the suspension rose to 60. Further, 3 mL of this inoculum was transferred to the autoclaved media under sterilized conditions and cultivated in a shaker (150 rpm) at 37 °C. The mycelium pellets having 2–3 mm diameter were formed spontaneously in 3 days.

2.3. Biosynthesis of CdS QDs

Following the formation of the ideal mycelium pellets, 137.5 mg of cadmium nitrate tetrahydrate, 10 mL of 0.668 g/L TAA, and 1 mL of TGA were added to the media with stirring. The pH values of the media in different flasks were adjusted to 9.0, 10.0, and 11.0 after which they were incubated at 37 °C on a rotary shaker (150 rpm). The color of the mycelial pellets changed from white to yellow after 12 h, which indicated that the QDs of CdS had been fabricated. This protocol could be used easily and reproducibly for the biosynthesis of the CdS nanocrystals.

2.4. Characterization

2.4.1. UV–vis and PL

Following cultivation at different pH conditions, the media containing *P. chrysosporium* from each Erlenmeyer flask was harvested by filtration with common qualitative filter papers to obtain the mycelial pellets. Then, the pellets were washed thrice with deionized water and suspended in centrifuge tubes with 30 mL deionized water followed by addition of 200 μL of TGA. Ultrasonic disruption of the cells was performed using an ultrasonic processor (XO-1000D, China) over three 45 s cycles at an interval of 3 s between the cycles. The sonicated samples were then centrifuged at 6000 × *g* for 10 min to precipitate the cell debris. The supernatant was collected for the measurement of UV–vis and PL spectra. Both the measurements were performed at room temperature. UV–vis absorption spectra were recorded on a Shimadzu UV-2550 spectrophotometer (Japan) whereas PL spectra were obtained with a Jobin–Yvon Horiba Fluoromax-4 spectrofluorimeter (HORIBA, Ltd., Japan).

2.4.2. Scanning electron microscopy (SEM) coupled with energy dispersive X-ray (EDX) analysis

The mycelial pellets were harvested by filtration after a 12 h incubation, washed thrice with deionized water, and then dried in a freezer dryer (FD-1, Boyikang, Beijing, China) below a temperature of −50 °C. The dry mycelial pellet (native, treated with cadmium ions) samples were treated with a gold sputtering and then measured on an SEM (FEI QUANTA-200, Holland FEI Company, Holland) equipped with an EDX. The micrographs were recorded and the corresponding EDX spectra were measured by focusing on selected area of nanocrystals.

2.4.3. FTIR, TG/DTA, and XRD

The lyophilized mycelial pellets (treated with cadmium ions) having adsorbed CdS nanocrystals were powdered and used for XRD analysis and TG/DTA. The XRD pattern was recorded using an automatic X-ray diffractometer (D8-Advance, Bruker Company, Germany). The TG/DTA graph was obtained from a Seiko TG/DTA comprehensive thermal analyzer (TG/DTA7300, Japan) under nitrogen protection. The FTIR spectra were determined in reflectance mode on a FTIR-8400S Spectrometer (SHIMADZU Corporation, Japan) by using KBr pellets of the powdered lyophilized mycelial pellets (native, treated with cadmium ions).

2.4.4. TEM

The harvested mycelium pellets (12 h, treated with cadmium ions) were washed thrice with deionized water and the CdS nanocrystals still attached to the mycelia were dispersed in water by ultrasonication. High-resolution TEM (HRTEM) was carried out

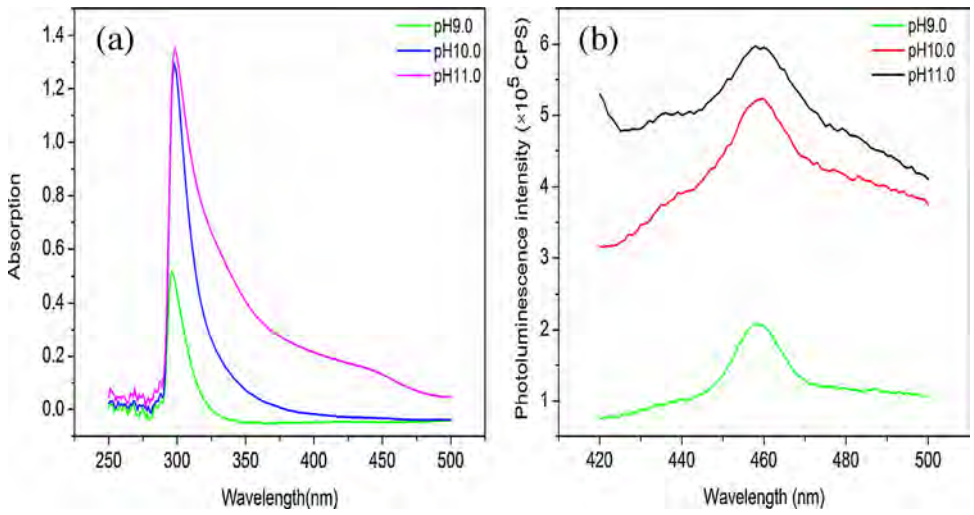

Fig. 1. (a) UV–vis and (b) PL spectra of extracellular biosynthesized CdS QDs following incubation with *P. chrysosporium* for 12 h. The maximum peak in the PL spectra was obtained at around 458 nm.

by placing a drop of aqueous solution containing CdS nanocrystals on a Lacey Support Film followed by air-drying. Transmission electron micrographs were obtained by using a FEI Tecnai G^2 F20 microscope operating at 200 kV (FEI company, USA).

2.5. Data analysis

All samples were analyzed in triplicate. The relative standard deviations (RSD) of our method for each type of data were less than 0.05.

3. Results and discussion

3.1. UV–vis analysis and PL spectra analysis

Extracellular biosynthesized CdS QDs were obtained under differing pH conditions. The growth was monitored and optical properties of the QDs were studied by recording the absorption and the PL spectra. The test QD samples were drawn from reaction vessels with differing pH values, and were centrifuged to remove fungal debris without further narrowing their size distribution. Each sample showed a well-resolved absorption maximum for the first electronic transition. The presence of the absorption peak from 296 to 298 nm is characteristic of CdS particles in the quantum size regime. The intensity of the absorption peak was progressively enhanced with an increase in the hydroxyl ion concentration, with an approximately 3-fold increase in the formation of nanoparticles at pH 11.0 compared to that at pH 9.0. Increased pH values were accompanied by a mild red shift of the absorption edge (Fig. 1a), indicating the growth of CdS QDs during the biochemical process [37].

The biosynthesized QDs yielded a strong fluorescence emission (Fig. 1b), and the PL emission spectra appeared excessively blue for CdS QDs, which implied that very small particles had been obtained. In terms of the procedure outlined in the literature [44], the average particle size of the biosynthesized QDs may be less than 3.0 nm as estimated from the spectra. Notably, all the full width at half maximum (FWHM) values of the PL curves were below 30 nm, which corresponded to narrow particle size distribution and superior monochromaticity. The UV–vis and PL results showed that CdS nanocrystals with good optical properties could be easily manufactured, and that increasing the pH may enhance production. Compared to the biosynthesis of emission-tunable cadmium selenide (CdSe) QDs in yeast cells [45], the harvesting of QDs was much easier with our extracellular synthesis approach using *P. chrysosporium*. The colloidal solution of CdS nanoparticles was extremely stable and did not show aggregation even after two months of storage.

3.2. XRD and TEM

In order to study the physicochemical properties of the nanocrystals, XRD and TEM were used to clarify the characteristics of phase properties, particle size, crystal system, and morphology. XRD provides extensive information about composition, internal atomic or molecular structure, and configuration of materials. The XRD pattern obtained for our typical CdS nanoparticle sample (Fig. 2) exhibited prominent broad peaks at 2θ values of 26.58°, 43.968°, and 52.138°, which could be indexed to the (1 1 1), (2 2 0), and (3 1 1) facets of the cubic phase CdS, respectively, according to JCPDS file no. 10-0454. The PDF card indicated that the nanoparticles were in line with the face-centered cubic crystal lattice having unit cell parameters: $a = b = c = 5.818$ belonging to space group $F\bar{4}3m(216)$.

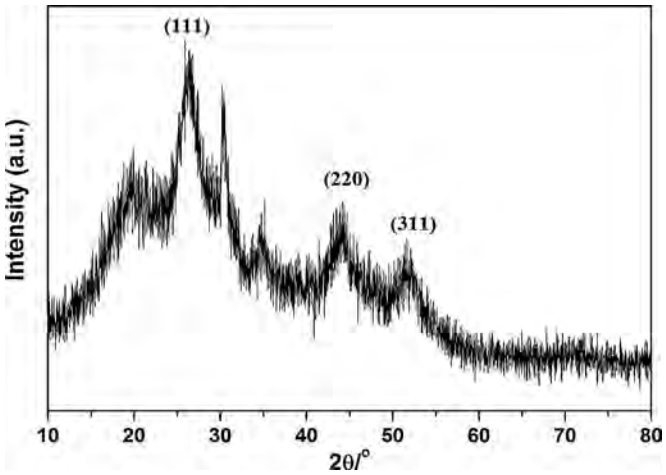

Fig. 2. XRD pattern of CdS nanoparticles. The peaks assigned to diffractions from the (1 1 1), (2 2 0), and (3 1 1) planes were of face-centered cubic CdS. The X-ray source was Cu Kα.

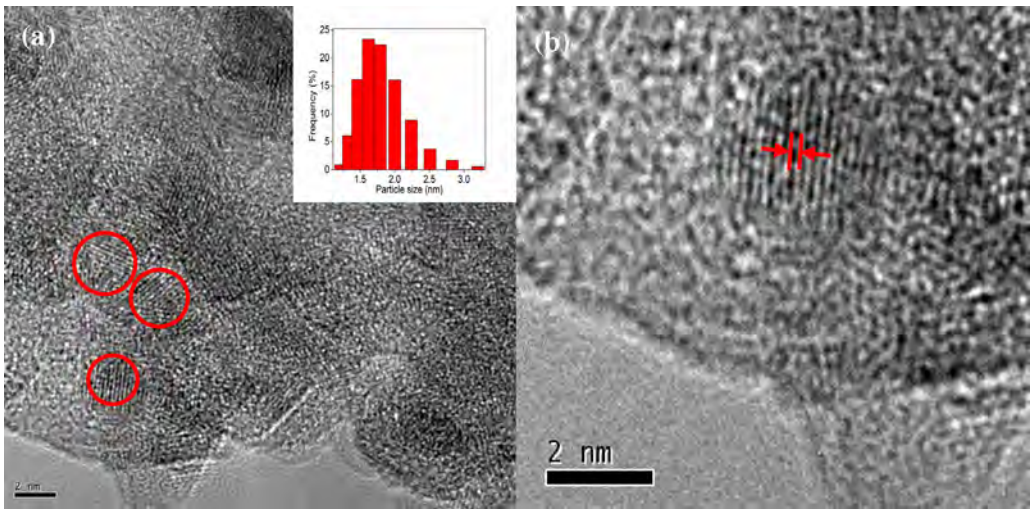

Fig. 3. (a) HRTEM images of extracellularly biosynthesized CdS QDs. (Inset) Size distribution of the QDs. (b) Expanded image of QDs. (2 2 0) lattice fringes of denoted area (d_{220} = 2.1 Å).

The average grain of the sample was determined to be approximately 2.56 nm, calculated from the FWHM of the most intense peak calculated with Scherrer's equation:

$$d = \frac{0.89\lambda}{\beta \cos\theta} \quad (1)$$

where λ is the wavelength of the X-ray radiation, β is the FWHM in radians of the XRD peak, and θ is the angle of diffraction.

The morphology and size of the CdS nanoparticles were observed by HRTEM. The TEM image (Fig. 3) showed uniform sphere-shaped nanoparticles, with sizes ranging from 1.5 to 2.0 nm. The inset particle size histogram showed an average particle size of 1.96 ± 0.1 nm. This value was approximately in agreement with the results estimated by PL and calculated by XRD. Fig. 3b further illustrated the lattice planes of the CdS nanocrystals, which showed a spacing of 0.21 nm corresponding to the d spacing of the (2 2 0) planes of the face-centered cubic (fcc) crystalline structure of CdS. The lattice planes in the HRTEM images were consistent with the XRD pattern (Fig. 2), which exhibited a relatively strong peak (~43.968°) indexed to the (2 2 0) planes of the standard pattern for cubic CdS. These findings indicated the biosynthesized CdS QDs were of a uniform size with good crystallinity.

3.3. TG/DTA

The lyophilized mycelial pellets which had formed CdS nanocrystals were powdered and used for TG/DTA analysis. As the TG curve indicated in Fig. 4, the weight of the sample dropped very quickly below 500 °C and the weight loss about 65% was due to the volatilization of water and gasification of the organic materials. The speed of decrease slowed down obviously over the period from 600 °C to 1300 °C (the upper temperature limit of TG analyzer). The weight loss was not manifest even when the temperature was above 1000 °C. Until the highest temperature of 1300 °C, there was still 10% of the weight existed, the residual should be the weight of CdS QDs. According to DTA analysis, an exothermal reaction should be occurred around 1200 °C. This point may be the onset temperature of degradation of the CdS nanoparticles. The TG/DTA analysis showed the good stability of CdS QDs.

3.4. SEM–EDX analysis

The dry mycelial pellets (native or cadmium ion-treated) were analyzed by SEM and EDX for a better understanding of the

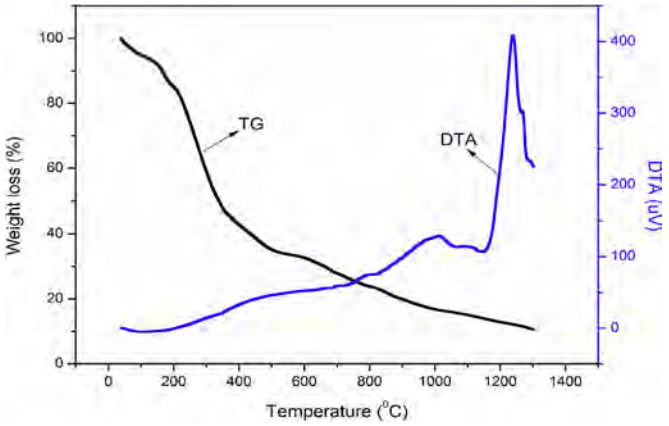

Fig. 4. TG/DTA analysis of CdS nanoparticles.

reaction process and to gain further insight into the features of the CdS nanoparticles. Through secondary electron signal imaging, the SEM technique showed the morphology of the samples and was used to observe the surface characteristics of *P. chrysosporium*. The SEM images of the native and cadmium ion-treated fungi were presented in Fig. 5. The surface of the native fungus appeared smooth and clear (Fig. 5a) without any adsorbed particles, while many light dots (cadmium binding particles) were dispersed on the mycelia surface (Fig. 5b). Picture c showed b in another imaging mode, highlighting the presence of a large number of nanoparticles that were absorbed on the mycelial surface. Picture f showed the energy spectra of region e in d. The EDX data shown in Fig. 5f confirmed the main elemental composition of carbon, oxygen, phosphorus, sulfur, and cadmium. The presence of the cadmium peak demonstrated that some cadmium ions were bound to the surface of the biomass.

Combining the results of XRD and TEM, we confirmed that the nanoparticles absorbed on the surface were CdS crystals. The peaks corresponding to carbon, oxygen, and phosphorus were characteristic of the composition of many organic substances in the cell wall of the biomass. The content of S was higher than that of Cd, plausibly because the cells release many other active sulfur-containing substances other than the sulfur contained in CdS. This analysis was similar to that described by Moreau, which showed that the sulfhydryl group present in cysteine and mercapto-compounds exhibit particularly strong specific binding to the surfaces of sulfide minerals and nanoparticles [46].

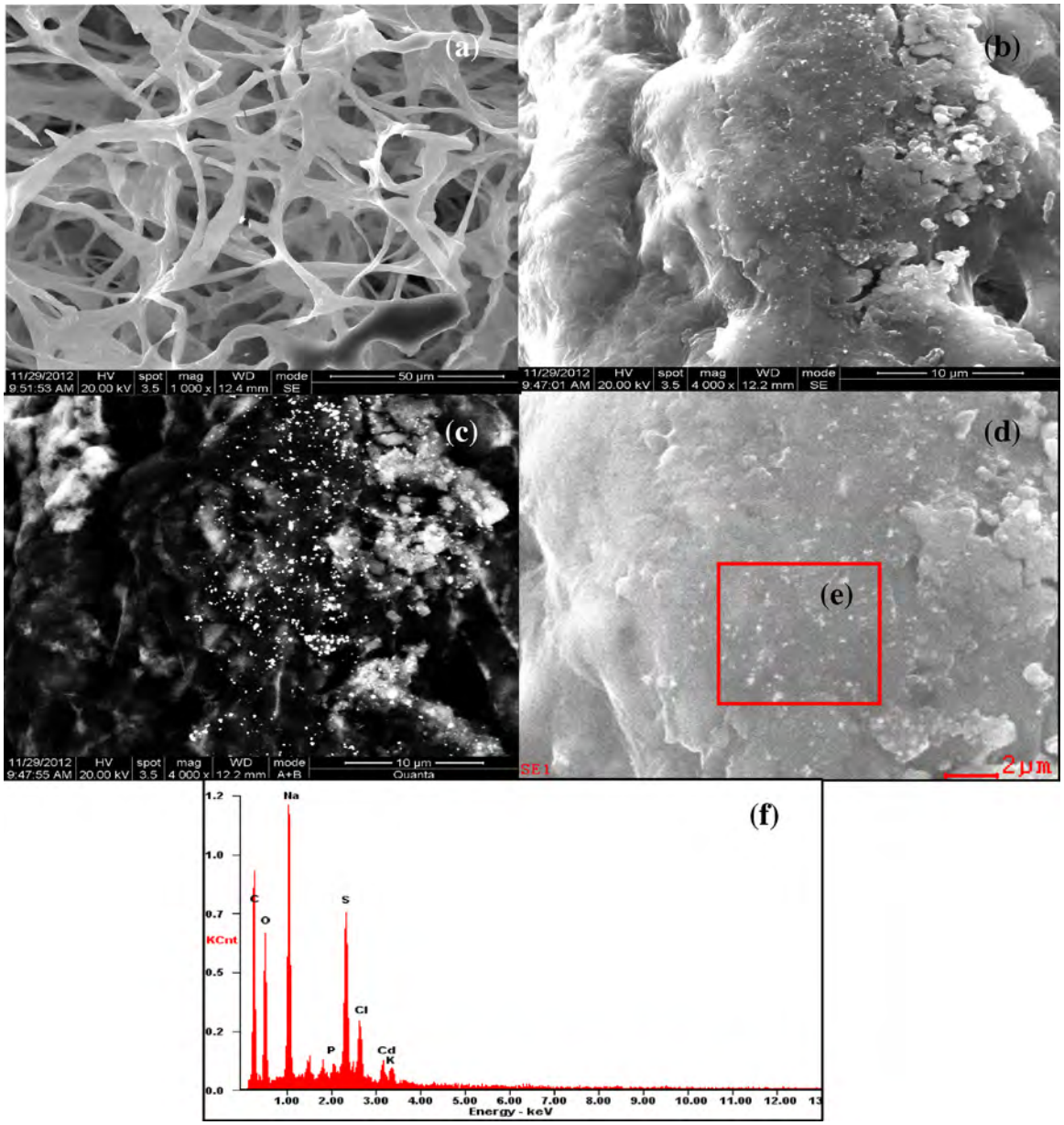

Fig. 5. SEM–EDX micrograph of mycelium pellets: (a) native; (b) and (c) treated with Cd(II); (d) expanded image of the nanocrystals in (b); (f) EDX graph of selected area (the red area in e). As observed from the graph, plenty of nanoparticles were adsorbed on the mycelia surface. (For interpretation of the references to color in this figure legend, the reader is referred to the web version of the article.)

Based on the analysis, it can be inferred that the *P. chrysosporium* mycelial surface is a superior place for the self-assembly of the CdS nanoparticles, and that the nanoparticles are a product of the physiological defense by the fungus against the toxic cadmium ions. Furthermore, cell secretions such as cysteines may play an important role in the process of synthesis.

3.5. FTIR

The mechanism of formation of the CdS nanoparticles was studied using the FTIR spectra of the native fungi and the Cd(II)-treated fungi. A number of absorption peaks belonging to several functional groups present in the fungal cell walls were detected in the FTIR spectrum (Fig. 6).

The strong, broad IR absorption band at around 3400 cm^{-1} for the native as well as the Cd(II)-treated fungus was characteristic of the O—H stretching vibration of the carboxyl group. In the 3500–3300 cm^{-1} region, the N—H stretching vibration bands of the fungal mass may overlap with the carboxyl group band [47]. The peaks observed at 2927 and 2858 cm^{-1} could be assigned to the anti-symmetric and symmetric vibrations of the $—CH_2$ groups of the hydrocarbons present in fungal protein. The spectra displayed two absorption peaks at 1640 and 1550 cm^{-1} corresponding to the stretching vibration of amide I (C═O) and the bending vibration of amide II (N—H) of the polypeptides or proteins, respectively [46]. The amide II band at 1550 cm^{-1}, belonging to the C—N stretching of O═C—N—H, also encompassed the asymmetric stretching vibration of COO— of the carboxylates [48]. The two bands at 1382 and 1040 cm^{-1} could be attributed to the C—N stretching vibrations of the aromatic and aliphatic amines, respectively. These facts suggest that biological molecules could possibly carry out the formation and stabilization of the CdS nanoparticles in an aqueous medium.

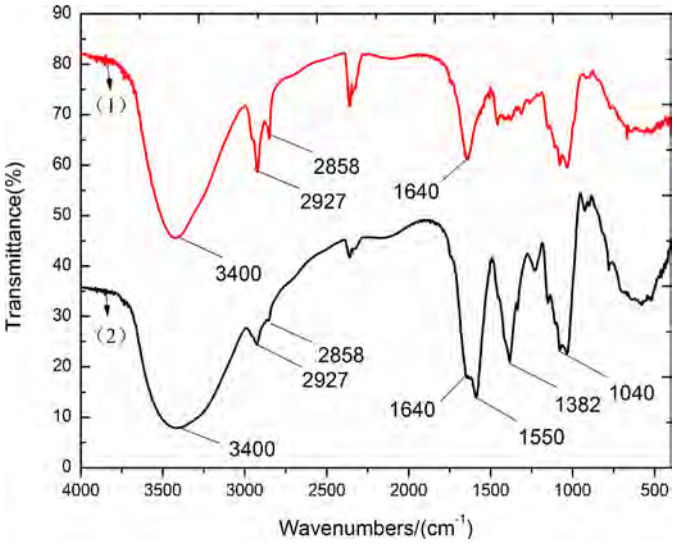

Fig. 6. IR spectra of *P. chrysosporium* (1) control and (2) exposed to Cd^{2+} for 12 h. The bands at 1640 and 1550 cm^{-1} were assigned to bending vibrations of the amide I and II bands, respectively. The two bands observed at 1382 and 1040 cm^{-1} could be due to the C—N stretching vibrations of the aromatic amines, respectively.

This result was in accordance with the finding that proteins can bind to gold nanoparticles either through their free amine groups, or through cysteine residues [49].

On comparison of the IR spectra, two significant differences were observed in the Cd(II)-treated fungi–broadening of the band at 3400 cm^{-1} corresponding to the O—H stretch vibration of the carboxyl group, and the appearance of a new band at 1550 cm^{-1} matching the —NH bending vibration of amide II. These two changes indicated that amino acids, proteins, or polypeptides, were secreted by the fungus. Taken together with the results from the EDX analysis, the secreted amino acids were probably cysteines. Thus, the amide and the carboxyl groups are possibly the critical factors in the synthesis of the CdS nanocrystals. As described by Gole and Sanghi, proteins may bind to nanoparticles either through free amine groups (those that do not react with carboxyl groups, or are uninvolved in the formation of the peptide chain), or through cysteine residues, via the electrostatic attraction of the negatively charged carboxylate groups of enzymes in the mycelial cell wall [49,50]. From the analyses, it appears the molecules secreted by the fungus possibly form a coat that covers the metal nanoparticles to prevent their agglomeration and aids their stabilization in the medium.

3.6. Mechanism

Presently, although a few reports on the microbial synthesis of nanoparticles are available, the most extensive researches were focused on the formation and properties of the products, while few studies have investigated the mechanisms for nanocrystal formation. Illustrating the molecular mechanism could enable better control over the process of biosynthesis, allowing the preparation of high quality materials.

Based on the results obtained from our study, a possible mechanism for the microbial synthesis of the face-centered CdS QDs has been put forth (Fig. 7). The CdS nanocrystals may be synthesized on the basis of the following chemical reactions:

$$Cd^{2+} + HS{-}R{-}COOH \rightarrow Cd{-}S{-}RCOOH + H^{+} \quad (a)$$

$$CH_3CSNH_2 + 3OH^{-} \leftrightarrow CH_3COO^{-} + NH_3 + S^{2-} + H_2O \quad (b)$$

$$Cd^{2+} + S^{2-} \rightarrow CdS \quad (c)$$

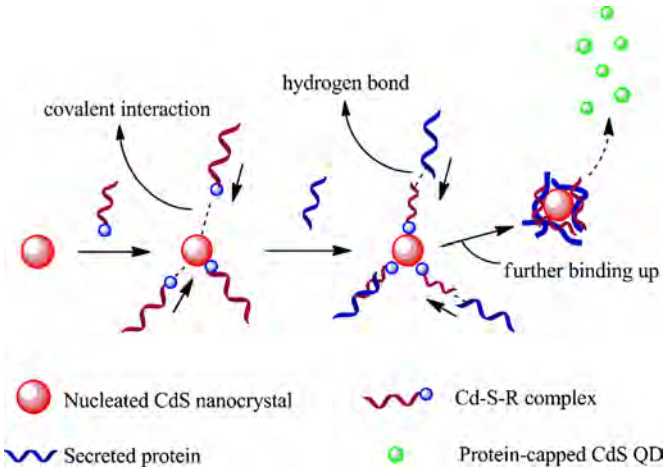

Fig. 7. Schematic representation of the mechanism for CdS QDs synthesis.

$$CdS + Cd{-}S{-}RCOOH \rightarrow CdSCd{-}S{-}RCOOH \quad (d)$$

$$CdSCd{-}S{-}RCOOH + NH_2CH(R)COOH \rightarrow CdSCd{-}S{-}RCOOH\cdots NH_2CH(R)COOH \quad (e)$$

At the outset, under stress due to the toxic heavy metal ion load, biomolecules such as cysteine and proteins may be secreted on the fungal cell wall surface, and these may capture cadmium ions via chelation with the thiol groups of cysteine. Further, the chelating compounds may be linked and form Cd-binding particles on the cell wall (Eq. (a)). Upon TAA hydrolysis, gradual release of S(II) into the solution (Eq. (b)) may occur, and these released ions may combine with the remaining cadmium ions to form CdS nuclei (Eq. (c)). The Cd—S—R complexes may then covalently bind to the CdS core [51] and form passivation layers (Eq. (d)), thereby producing CdS nanocrystals. At the same time, other carboxylic acid-containing biomolecules such as proteins or polypeptides, which also have the capacity to assemble on the surface of CdS nanocrystals (Eq. (e)), may in turn be responsible for capping the CdS nanocrystals via hydrogen bonding and electrostatic interactions [41]. Through the steps described above, tiny monodispersed nanocrystals may be manufactured. The capped masses on the surface may be of significance for the monodispersity of the CdS nanocrystals. More research needs to be carried out to confirm the mechanism proposed above.

4. Conclusions

In this study, the white rot fungus *P. chrysosporium* was used for the successful synthesis of fluorogenic CdS nanoparticles. TEM analysis revealed a uniform morphology and good crystallinity. The XRD pattern confirmed the "fcc" crystalline structure of metallic CdS. A good stability was shown by TG/DTA analysis. Using Scherer's equation, the average size was estimated to be approximately 2.56 nm, corresponding with the results of the TEM and PL analyses. The PL spectra showed a pure blue emission with an FWHM narrower than 30 nm, indicating good optical properties. EDX and FTIR analyses revealed the important role played by proteins and amino acids during the process of formation of the CdS nanocrystals. Thus, the superior optical properties and low toxicity of the biosynthesized CdS QDs make them extremely useful for bio-imaging and bio-labeling applications. In addition, the mechanisms discussed in this article may be of great use for the extracellular biosynthesis and size control of metal nanoparticles.

Acknowledgments

This study was financially supported by the National Natural Science Foundation of China (51178171, 51108166, 51039001), the Program for New Century Excellent Talents in University (NCET-10-0361), the Hunan Provincial Natural Science Foundation of China (10JJ7005), and the Scholarship Award for Excellent Doctoral Student granted by the Ministry of Education.

References

[1] A.P. Alivisatos, Perspectives on the physical chemistry of semiconductor nanocrystals, J. Phys. Chem. 100 (1996) 13226–13239.
[2] A.P. Alivisatos, Semiconductor clusters, nanocrystals, and quantum dots, Science 271 (1996) 933–937.
[3] C.B. Murray, D.J. Norris, M.G. Bawendi, Synthesis and characterization of nearly monodisperse CdE (E = S, Se, Te) semiconductor nanocrystallites, J. Am. Chem. Soc. 115 (1993) 8706–8715.
[4] X.G. Peng, L. Manna, W.D. Yang, J. Wickham, E. Scher, A. Kadavanich, et al., Shape control of CdSe nanocrystals, Nature 404 (2000) 59–61.
[5] L. Manna, E.C. Scher, A.P. Alivisatos, Shape control of colloidal semiconductor nanocrystals, J. Cluster Sci. 13 (2002) 521–532.
[6] Y.G. Zheng, Z.C. Yang, J.Y. Ying, Aqueous synthesis of glutathione-capped ZnSe and Zn1–*x*Cd*x*Se alloyed quantum dots, Adv. Mater. 19 (2007) 1475–1479.
[7] C. Chen, et al., Quantum dots-based immunofluorescence technology for the quantitative determination of HER2 expression in breast cancer, Biomaterials 30 (2009) 2912–2918.
[8] N.M. Idris, Z.Q. Li, L. Ye, E.K.W. Sim, R. Mahendran, P.C.L. Ho, et al., Tracking transplanted cells in live animal using upconversion fluorescent nanoparticles, Biomaterials 30 (2009) 5104–5113.
[9] N.P. Gaponik, D.V. Talapin, A.L. Rogach, A light-emitting device based on a CdTe nanocrystal/polyaniline composite, Phys. Chem. Chem. Phys. 1 (1999) 1787–1789.
[10] W.U. Huynh, J.J. Dittmer, A.P. Alivisatos, Hybrid nanorod-polymer solar cells, Science 295 (2002) 2425–2427.
[11] J.M. Liu, L.P. Lin, L. Jiao, M.L. Cui, X.X. Wang, L.H. Zhang, Z.Y. Zheng, CdS/TiO_2–fluorescein isothiocyanate nanoparticles as fluorescence resonance energy transfer probe for the determination of trace alkaline phosphatase based on affinity adsorption assay, Talanta 98 (2012) 137–144.
[12] K. Tomihira, D.G. Kim, M. Nakayama, Photoluminescence dynamics of energy transfer between CdS quantum dots prepared by a colloidal method, J. Lumin. 122/123 (2007) 471–473.
[13] P. Li, C.W. Zhang, J. Lian, S. Gao, X. Wang, First-principles study on electronic and magnetic properties of Cu-doped CdS, Solid State Commun. 151 (2011) 1712–1715.
[14] Y.J. Yang, X. Tao, Q. Hou, J.F. Chen, Fluorescent mesoporous silica nanotubes incorporating CdS quantum dots for controlled release of ibuprofen, Acta Biomater. 5 (2009) 3488–3496.
[15] A.D. Saran, J.R. Bellare, Green engineering for large-scale synthesis of water-soluble and bio-taggable CdSe and CdSe–CdS quantum dots from microemulsion by double-capping, Colloids Surf. A 369 (2010) 165–175.
[16] Y.J. Bao, J.J. Li, Y.T. Wang, L. Yu, J. Wang, W.J. Du, L. Lou, Z.Q. Zhu, H. Peng, J.Z. Zhu, Preparation of water soluble CdSe and CdSe/CdS quantum dots and their uses in imaging of cell and blood capillary, Opt. Mater. 34 (2012) 1588–1592.
[17] C.C. Mi, Y.Y. Wang, J.P. Zhang, H.Q. Huang, L.R. Xu, S. Wang, X.X. Fang, J. Fang, C.B. Mao, S.K. Xu, Biosynthesis and characterization of CdS quantum dots in genetically engineered *Escherichia coli*, J. Biotechnol. 153 (2011) 125–132.
[18] A. Akbarzadeh, D. Zare, A. Farhangi, M.R. Mehrabi, D. Norouzian, S. Tangestaninejad, M. Moghadam, N. Bararpour, Synthesis and characterization of gold nanoparticles by tryptophane, Am. J. Appl. Sci. 6 (2009) 691–695.
[19] K.S. Tapan, L.R. Andrey, Nonspherical noble metal nanoparticles: colloid chemical synthesis and morphology control, Adv. Mater. 21 (2009) 1–24.
[20] X.L. Zhang, S. Yan, R.D. Tyagi, R.Y. Surampalli, Synthesis of nanoparticles by microorganisms and their application in enhancing microbiological reaction rates, Chemosphere 82 (2011) 489–494.
[21] D.W. Wei, W.P. Qian, Facile synthesis of Ag and Au nanoparticles utilizing chitosan as a mediator agent, Colloids Surf. B 62 (2008) 136–142.
[22] B.R. Peelle, E.M. Krauland, K.D. Wittrup, A.M. Belcher, Design criteria for engineering inorganic material-specific peptides, Langmuir 21 (2005) 6929–6933.
[23] N. Ma, C.J. Dooley, S.O. Kelley, RNA-templated semiconductor nanocrystals, J. Am. Chem. Soc. 128 (2006) 12598–12599.
[24] K.T. Nam, D.W. Kim, P.J. Yoo, C.Y. Chiang, N. Meethong, P.T. Hammond, Y.M. Chiang, A.M. Belcher, Virus-enabled synthesis and assembly of nanowires for lithium ion battery electrodes, Science 312 (2006) 885–888.
[25] A. Anshup, J.S. Venkataraman, C. Subramaniam, R.R. Kumar, S. Priya, T.R.S. Kumar, R.V. Omkumar, A. John, T. Pradeep, Growth of gold nanoparticles in human cells, Langmuir 21 (2005) 11562–11567.
[26] L.W. Du, H. Jiang, X.H. Liu, E.K. Wang, Biosynthesis of gold nanoparticles assisted by *Escherichia coli* DH5α and its application on direct electrochemistry of hemoglobin, Electrochem. Commun. 9 (2007) 1165–1170.
[27] C.B. Mao, C.E. Flynn, A. Hayhurst, R. Sweeney, J.F. Qi, G. Georgiou, B. Belcher, A.M. Iverson, Viral assembly of oriented quantum dot nanowires, Proc. Natl. Acad. Sci. U.S.A. 100 (2003) 6946–6951.
[28] P.J. Yoo, K.T. Nam, J. Qi, S.K. Lee, J. Park, A.M. Belcher, P.T. Hammond, Spontaneous assembly of viruses on multilayered polymer surfaces, Nat. Mater. 5 (2006) 234–240.
[29] Y. Huang, C.Y. Chiang, S.K. Lee, Y. Gao, E.L. Hu, J.D. Yoreo, A.M. Belcher, Programmable assembly of nanoarchitectures using genetically engineered viruses, Nano Lett. 5 (2005) 1429–1434.
[30] P. Ngweniform, D. Li, C.B. Mao, Self-assembly of drug-loaded liposomes on genetically engineered protein nanotubes: a potential anti-cancer drug delivery vector, Soft Matter 5 (2009) 954–956.
[31] K. Kalishwaralal, V. Deepak, S.R.K. Pandian, S. Gurunathan, Biological synthesis of gold nanocubes from *Bacillus licheniformis*, Bioresour. Technol. 100 (2009) 5356–5358.
[32] N. Vigneshwaran, A.A. Kathe, P.V. Varadarajan, R.P. Nachane, R.H. Balasubramanya, Biomimetics of silver nanoparticles by white rot fungus, *Phanerochaete chrysosporium*, Colloids Surf. B 53 (2006) 55–59.
[33] A.V. Kirthi, A.A. Rahuman, C. Jayaseelan, L. Karthik, S. Marimuthu, T. Santhoshkumar, J. Venkatesan, S.K. Kim, G. Kumar, S.R.S. Kumar, K.V.B. Rao, Novel approach to synthesis silver nanoparticles using plant pathogenic fungi, *Puccinia graminis*, Mater. Lett. 81 (2012) 69–72.
[34] R.S. Ahmad, F. Ali, R.S. Hamid, M. Sara, Synthesis and effect of silver nanoparticles on the antibacterial activity of different antibiotics against *Staphylococcus aureus* and *Escherichia coli*, Nanomed. Nanotechnol. 3 (2007) 168–171.
[35] S. Minaeian, A.R. Shahverdi, A.S. Nohi, H.R. Shahverdi, Extracellular biosynthesis of silver nanoparticles by some bacteria, J. Sci. IAU (JSIAU) 17 (2008) 1–4.
[36] N. Mokhtari, S. Daneshpajouh, S. Seyedbagheri, R. Atashdehghan, K. Abdi, S. Sarkar, S. Minaian, H.R. Shahverdi, A.R. Shahverdi, Biological synthesis of very small silver nanoparticles by culture supernatant of *Klebsiella pneumonia*: the effects of visible-light irradiation and the liquid mixing process, Mater. Res. Bull. 44 (2009) 1415–1421.
[37] H.F. Bao, Z.S. Lu, X.Q. Cui, Y. Qiao, J. Guo, J.M. Anderson, C.M. Li, Extracellular microbial synthesis of biocompatible CdTe quantum dots, Acta Biomater. 6 (2010) 3534–3541.
[38] A. Ahmad, P. Mukherjee, D. Mandal, S. Senapati, M.I. Khan, R. Kumar, et al., Enzyme mediated extracellular synthesis of CdS nanoparticles by the fungus, *Fusarium oxysporum*, J. Am. Chem. Soc. 124 (2002) 12108–12109.
[39] M. Kowshik, N. Deshmukh, W. Vogel, J. Urban, S.K. Kulkarni, K.M. Paknikar, Microbial synthesis of semiconductor CdS nanoparticles, their characterization, and their use in the fabrication of an ideal diode, Biotechnol. Bioeng. 78 (2002) 583–588.
[40] H.J. Bai, Z.M. Zhang, Y. Guo, G.E. Yang, Biosynthesis of cadmium sulfide nanoparticles by photosynthetic bacteria *Rhodopseudomonas palustris*, Colloids Surf. B 70 (2009) 142–146.
[41] R. Sanghi, P. Verma, A facile green extracellular biosynthesis of CdS nanoparticles by immobilized fungus, Chem. Eng. J. 155 (2009) 886–891.
[42] R.Y. Sweeney, C.B. Mao, X.X. Gao, J.L. Burt, A.M. Belcher, G. Georgiou, et al., Bacterial biosynthesis of cadmium sulfide nanocrystals, Chem. Biol. 11 (2004) 1553–1559.
[43] H.J. Bai, Z.M. Zhang, J. Gong, Biological synthesis of semiconductor zinc sulfide nanoparticles by immobilized *Rhodobacter sphaeroides*, Biotechnol. Lett. 28 (2006) 1135–1139.
[44] W.W. Yu, L.H. Qu, W.Z. Guo, X.G. Peng, Experimental determination of the extinction coefficient of CdTe, CdSe, and CdS nanocrystals, Chem. Mater. 15 (2003) 2854–2860.
[45] R. Cui, et al., Living yeast cells as a controllable biosynthesizer for fluorescent quantum dots, Adv. Funct. Mater. 19 (2009) 2359–2364.
[46] J.W. Moreau, P.K. Weber, M.C. Martin, B. Gilbert, I.D. Hutcheon, J.F. Banfield, Extracellular proteins limit the dispersal of biogenic nanoparticles, Science 316 (2009) 1600–1603.
[47] S.B. Choi, Y.S. Yun, Biosorption of cadmium by various types of dried sludge: an equilibrium study and investigation of mechanisms, J. Hazard. Mater. 138 (2006) 378–383.
[48] R. Sanghi, N. Sankararamakrishnan, B.C. Dave, Fungal bioremediation of chromates: conformational changes of biomass during sequestration, binding, and reduction of hexavalent chromium ions, J. Hazard. Mater. 169 (2009) 1074–1080.
[49] A. Gole, C. Dash, V. Ramachandran, S.R. Sainkar, A.B. Mandale, M. Rao, M. Sastry, Pepsin-gold colloid conjugates: preparation, characterization, and enzymatic activity, Langmuir 17 (2001) 1674–1679.
[50] R. Sanghi, P. Verma, Biomimetic synthesis and characterisation of protein capped silver nanoparticles, Bioresour. Technol. 100 (2009) 501–504.
[51] H.X. Tang, M. Yan, H. Zhang, M.Z. Xia, D.R. Yang, Preparation and characterization of water-soluble CdS nanocrystals by surface modification of ethylene diamine, Mater. Lett. 59 (2005) 1024–1027.